LAWRENCE
LIVERMORE
NATIONAL
LABORATORY

UCRL-CONF-232468

Tomography and Methods of Travel-Time Calculation for Regional Seismic Location

S.C. Myers, S. Ballard, C. Rowe, G. Wagoner, M. Antolik, S. Phillips, A. Ramirez, M. Begnaud, M. E. Pasyanos, D. A. Dodge, M. P. Flanagan, K. Hutchenson, G. Barker, J. Dwyer, D. Russell

July 3, 2007

MRR2007 - 29th Research Review on Nuclear Explosion Monitoring Technologies
Denver, CO, United States
September 25, 2007 through September 27, 2007

Disclaimer

TOMOGRAPHY AND METHODS OF TRAVEL-TIME CALCULATION FOR REGIONAL SEISMIC LOCATION

Stephen C. Myers[1], Sanford Ballard[2], Charlotte Rowe[3], Gregory Wagner[4], Michael Antolik[5], Scott Phillips[2], Abe Ramirez[1], Mike Begnaud[2], Mike Pasyanos[1], Doug Dodge[1], Megan Flanagan[1], Kevin Hutchenson[5], Glenn Barker[2], John Dwyer[4], and David Russell[4]

[1]Lawrence Livermore National Laboratory, [2]Sandia National Laboratory, [3]Los Alamos National Laboratory, [4]Air Force Technical Applications Center, [5]Quantum Technology Sciences, Inc.

Sponsored by National Nuclear Security Administration
Office of Nonproliferation Research and Development
Office of Defense Nuclear Nonproliferation

ABSTRACT

We are developing a laterally variable velocity model of the crust and upper mantle across Eurasia and North Africa to reduce event location error by improving regional travel-time prediction accuracy. The model includes both P and S velocities and we describe methods to compute travel-times for Pn, Sn, Pg, and Lg phases. For crustal phases Pg and Lg we assume that the waves travel laterally at mid-crustal depths, with added ray segments from the event and station to the mid crustal layer. Our work on Pn and Sn travel-times extends the methods described by Zhao and Xie (1993). With consideration for a continent-scale model and application to seismic location, we extend the model parameterization of Zhao and Xie (1993) by allowing the upper-mantle velocity gradient to vary laterally. This extension is needed to accommodate the large variation in gradient that is known to exist across Eurasia and North African. Further, we extend the linear travel-time calculation method to mantle-depth events, which is needed for seismic locators that test many epicenters and depths. Using these methods, regional travel times are computed on-the-fly from the velocity model in milliseconds, forming the basis of a flexible travel time facility that may be implemented in an interactive locator.

We use a tomographic technique to improve upon a laterally variable starting velocity model that is based on Lawrence Livermore and Los Alamos National Laboratory model compilation efforts. Our tomographic data set consists of approximately 50 million regional arrivals from events that meet the ground truth (GT) criteria of Bondar *et al*. (2004) and other non-seismic constraints. Each datum is tested to meet strict quality control standards that include comparison with established distance-dependent travel-time residual populations relative to the IASPIE91 model. In addition to bulletin measurements, nearly 50 thousand arrival measurements were made at the national laboratories. The tomographic method adjusts Pn velocity, mantle gradient, and a node-specific crustal slowness correction for optimized travel-time prediction.

OBJECTIVES

This project produces a laterally variable velocity model of the crust and upper mantle that is specifically designed for use in routine seismic location. At this time the Seismic Location Baseline Model (SLBM) is focused on travel-time prediction at local and regional distances. Therefore, ray paths are wholly within the crust and upper mantle. Like any travel-time prediction method used in a location algorithm the SLMB must return:

1. An accurate travel-time prediction

2. An uncertainty estimate of the travel-time prediction error

Because the SLBM is meant for use in routine location algorithms where networks can be dynamic and pre-computation of travel-times for all available data may not be possible, the SLBM must also

3. Compute the travel-time on-the-fly given regional- or local-distance station/event coordinates.

4. Return the travel-time in milliseconds, thus enabling the estimation of a location in a few seconds

Further, we aim to improve a starting model that is based on a geophysical compilation. The improvement will be achieved using a ground-truth data set and a tomographic technique that is tailored to optimize model parameters important to seismic location.

RESEARCH ACCOMPLISHED

We meet the objectives outline above by adapting several approaches for model parameterization and travel-time calculation into one package for computation of regional- and local-distance travel-times for Pn, Sn, Pg, and Lg phases.

A challenge for this project is developing a model parameterization that enables fast and accurate prediction of each local/regional phase at all applicable distances. Well-established methods can be used to compute regional Pn and Sn travel-times (e.g. Hearn, 1984), but the accuracy of these methods degrades at far regional (>1000 km) distance (e.g. Hearn et al., 2004). To more accurately predict Pn and Sn at far-regional distances, Zhao (1993) and Zhao and Xie (1993) approximation upper-mantle structure with a linear gradient, resulting in a simple expression for calculating travel time. For Pn and Sn, we adapt the Zhao and Xie (1993) approach for application to seismic location. For Pg and Lg (Sg) at local distances, we extract a vertical cross section from the model and use 2-dimensional ray tracing to compute the travel time. At regional distance, we approximate the crustal waveguide with a laterally variable velocity layer, while accounting for propagation to/from the event/station using ray tracing.

In each instance we use tomographic methods to improve travel-time prediction of the model. Lawrence Livermore and Los Alamos National Laboratories develop a joint ground truth data set and apply stringent quality control measures on arrival-time measurement to produce a high quality tomographic data set. We adapt Pn tomographic methods (e.g Hearn 2004; Zhao and Xie, 1993, Phillips et al, 2007) to improve travel-time predictions of regional phases.

Model parameterization

We combine the laterally variable layer approach of Pasyanos et al. (2004) with the linear mantle gradient of Zhao and Xie (1993). Layer definitions are specified in Table 1. Note that the thickness of some layers may be zero. For instance, on the continents the depth of the water layer coincides with the depth of the model layer exposed at the surface. Velocity vs. depth profiles are defined at nodes, and the profiles at the nodes are interpolated to determine velocity at any arbitrary location (lat,lon,depth). The node structure is a tessellation on a sphere with node spacing of approximately 1° (Figure 1). At present, the model development domain is Eurasia and North Africa, and nodes outside of that domain are set to a default velocity profile based on iasp91 (Kennett and Engdahl, 1991). This parameterization provides a seamless and extensible model. Expansion beyond Eurasia and North Africa does not require a change in the model

parameterization itself, only modification of the velocity structure at a given node. The model incorporates the GRS84 ellipsoid, eliminating the need for the conventional ellipticity correction to travel-time predictions.

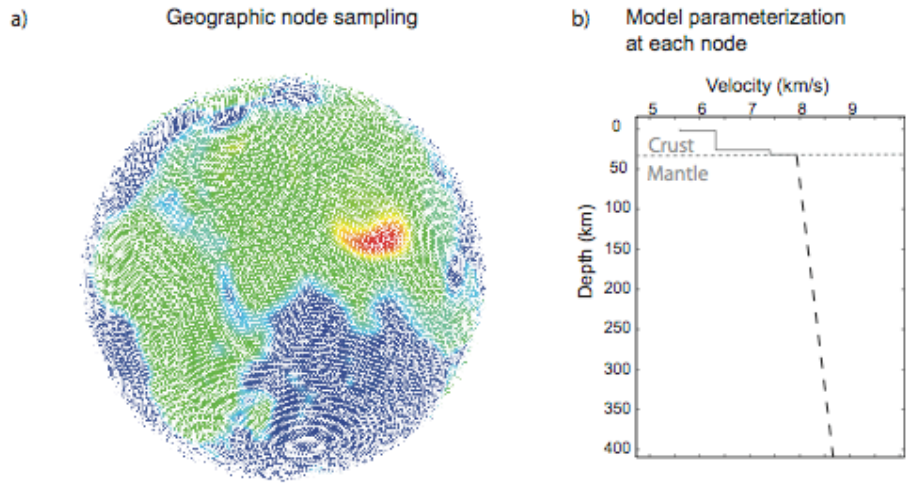

Figure 1. Seismic Location Baseline Model (SLBM) global parameterization. a) An example tessellation with approximately 1° grid spacing. Color is based on approximate Moho depth. b) An example velocity/depth profile as defined at each node. The mantle portion of the profile is specified by the velocity at the crust/mantle interface and a linear gradient.

Table 1. Model entities and associated parameters. Depths and velocities at each node are interpolated to define a 3-dimensional crustal model that overlies a laterally variable model in the shallow mantle. Note that the mid crustal layer is distinct, in that the velocities are specified individually for each phase. For Pn and Sn the mid-crustal layer is used in conjunction with all other crustal layers to compute travel-times for rays that travel steeply through the crust. For Pg and Lg distinct middle crust velocities are used to model the horizontal slowness of the regional phases that are trapped in the crust.

Model entity	Layer Depth	P-wave velocity	S-wave velocity	P-wave gradient	S-wave gradient
Water	Yes	Yes	Yes		
Sediment 1	Yes	Yes	Yes		
Sediment 2	Yes	Yes	Yes		
Sediment 3	Yes	Yes	Yes		
Upper Crust	Yes	Yes	Yes		

Model entity	Layer Depth	P-wave velocity	S-wave velocity	P-wave gradient	S-wave gradient
Middle Crust	Yes	Independent for Pn, Pg	Independent for Sn, Lg		
Lower Crust	Yes	Yes	Yes		
Moho	Yes	Yes	Yes		
Mantle Gradient				Yes	Yes

Travel-time calculation, Pn and Sn

The travel-time calculation is based on the method described in Zhao (1993) and Zhao and Xie (1993). This calculation is similar to the widely used approach of Hearn (1984), with an additional term (γ) introduced to account for diving rays that may occur due to a positive velocity gradient with depth and Earth sphericity. The travel-time calculation is

$$TT = \sum_{i=1}^{N} d_i s_i + \alpha + \beta + \gamma \qquad [1]$$

where *d* and *s* are the distance and slowness (taken as 1/MohoVelocity) in each of the *i* segments comprising the great-circle path from Moho pierce points near the event and station, α and β are the crustal travel times at the source and receiver, and γ is a term that accounts for the effect of both mantle velocity gradient and earth sphericity.

We define α as:

$$\alpha = \sum_{j=1}^{M} \left[\sqrt{r_j^2 / v_j^2 - p^2} - \sqrt{r_{j+1}^2 / v_j^2 - p^2} \right] \qquad [2]$$

where *v* and *r* are the velocity and layer radius of the *M* crustal layers from the event to the Moho, and *p* is the ray parameter ($p=1/v$, *v* evaluated at the ray bottoming depth).

We similarly define β as:

$$\beta = \sum_{k=1}^{N} \left[\sqrt{r_k^2 / v_k^2 - p^2} - \sqrt{r_{k+1}^2 / v_k^2 - p^2} \right] \qquad [3]$$

where *v* and *r* are defined as above for the *L* crustal layers from the station to the Moho. The same p is used in both Eqns [2] and [3]. Because the ray bottoming depth is a function of the pierce point, p is determined through an efficient, iterative process.

Per Zhao (1993),

$$\gamma = -\frac{c^2 Xm^3}{24 V_0} \qquad [4]$$

where X_m is the horizontal distance traveled in the mantle, c is a velocity gradient in the mantle that is normalized by the velocity a crust mantle boundry plus an additional term to account for earth sphericity (Helmberger, 1973), and V_0 is a regional average of Pn velocity over the entire study area.

We introduce spatially varying *c* into the model (Phillips et al., 2007), and we calculate γ by averaging c along each ray. V_0 remains an average Pn velocity over the whole model, which allows us to take advantage of linear tomographic inversion methods (see below). Tests suggest that the approximation to V_0 introduces negligible travel-time error given Pn velocities ranging from 7.5 km/s to 8.3 km/s.

The Zhao (1993) method is applicable to events in the crust, and for nuclear explosion monitoring we are primarily interested in crustal events. However, seismic location algorithms may explore the possibility that an event occurred in the mantle, making travel-time predictions for mantle events desirable. The following extends the travel-time method to events in the shallow mantle, with the condition that $c^2h^2 \ll 1$ (h is the bottoming depth of the ray).

$$TT = \alpha + t_m \qquad [5]$$

where α is the crustal travel time from the Moho to the station (as defined in [2]), and t_m is the travel time in the mantle. Figure 2 shows the geometry and defines many of the variables used in the following equation.

$$t_m = \frac{\left[t_{Moho}\frac{x_m}{d} - \left(\frac{c^2 x_m^2}{24 V_0}\right)\right] \pm \left[t_{Moho}\left(\frac{x_z}{d(1+c_m z_m)}\right) - \left(\frac{c^2 x_z^2}{24 V_{0z}}\right)\right]}{2} \qquad [6]$$

If the ray leaves the event upwards, then the second term is subtracted. If the ray leaves the event downwards, then the second term is added. t_{Moho} is the travel time for a ray traversing the Moho from the event to the point where the ray enters the crust and propagates to the station. x_m is the horizontal distance as measured at Moho radius by a ray that starts at the Moho then travels downward passing through the event and continuing to the station. x_z is similar to x_m, but the horizontal distance is measured at the radius of the event. d is the horizontal distance traveled in the mantle from the event to the Moho pierce point below the station, as measured at Moho radius. c_m is the mantle velocity gradient normalized by average Moho velocity, with the addition of a term to account for earth sphericity (Helmberger, 1973). z_m is the depth of the event below the Moho. V_{oz} is the average model velocity at the depth of the event.

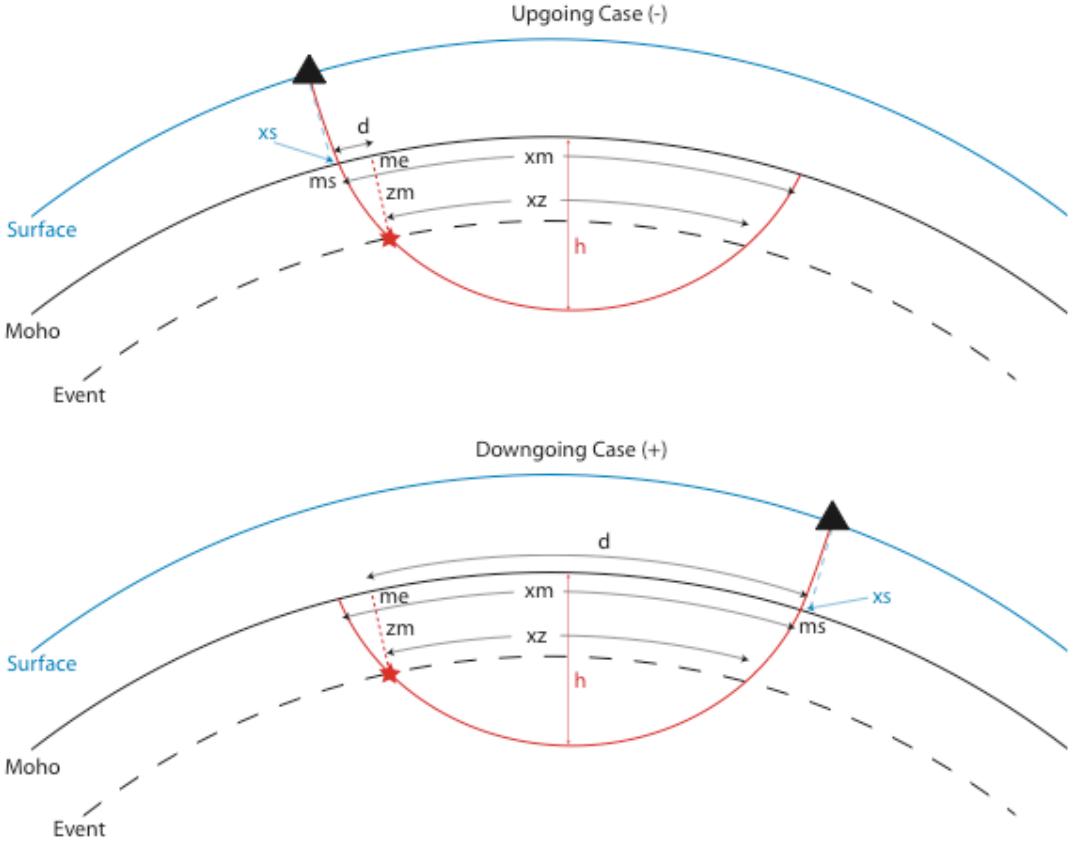

Figure 2. Geometry and variable definition extending the Zhao and Xie (1993) formulation to events in the shallow mantle. The red star is the event location and the triangle is the station location.

Travel-time calculation, Pg and Lg

Both Pg and Lg phases are trapped in the crust, and both phases exhibit complex waveforms that require hundreds or thousands of rays to model. Further, the first arriving ray with sufficient energy to be observed is dependent on geologic structure and event-station distance. Therefore, it is difficult to physically model the observed travel time using conventional ray techniques. Empirically, Pg and Lg travel at horizontal velocities of approximately 6.0 km/s and 3.2 km/s (respectively), which is suggestive of propagation in the middle crust. Further, studies suggest that event depth can impart a static travel-time delay, suggesting a component of propagation from the event to the middle crust then up to the station. We capture this travel-time behavior with a simple approximation whereby:

$$TT = \sum_{i=1}^{N} d_i s_i + \alpha + \beta \qquad [7]$$

where d_i is the distance traveled in the middle crust in each of N ray segments, α and β propagate the phase to and from the middle crust, respectively. When the source is above the middle crust, then the calculation is almost the same as [1], but the correction for a diving ray is not used. When the source is below the mid-crustal layer, we assume that the ray travels horizontally until Earth sphericity causes the ray to intersect the mid crustal layer. While this approach by no means captures the physical complexity of Pg and Lg wave propagation, we find that this approach is suitable for estimating travel-time.

Computational efficiency

Travel-time facilities used in routine location algorithms must be computationally efficient. Analysts often iterate on arrival-time determinations, first locating the event with clear arrivals, then adding additional arrivals (or adjusting previous measurements) based on a preliminary location. Analysts can not waste time waiting for the calculation of a location before continuing work. Considering that a location requires the computation of travel times for many phase, over many iterations, often with numerical calculation of derivatives (at least 4 travel-time calculations per observation per iteration), the time to compute an individual travel-time must be negligible (milliseconds).

The algebraic form of the travel-time formulas that are specified above consume negligible computer time. The primary challenge is fast extraction of the information from the laterally variable model into a cross sectional profile needed for the travel-time calculation. The tessellation model parameterization takes advantage of mature algorithms to determine which triangle any given point lies within, which nodes comprise the triangle, and node weights used for interpolation. Figure 3 shows an example of a cross section and the Pn ray that is used to compute the travel time.

Test results show a linear increase in computer time as a function of event-station distance. In the distance range from ~200 km to ~2200 km, Pn/Sn travel-times require ~2 milliseconds to ~10 milliseconds to compute on a desktop computer with ~1.5Ghz clock speed. Pg/Lg times are faster.

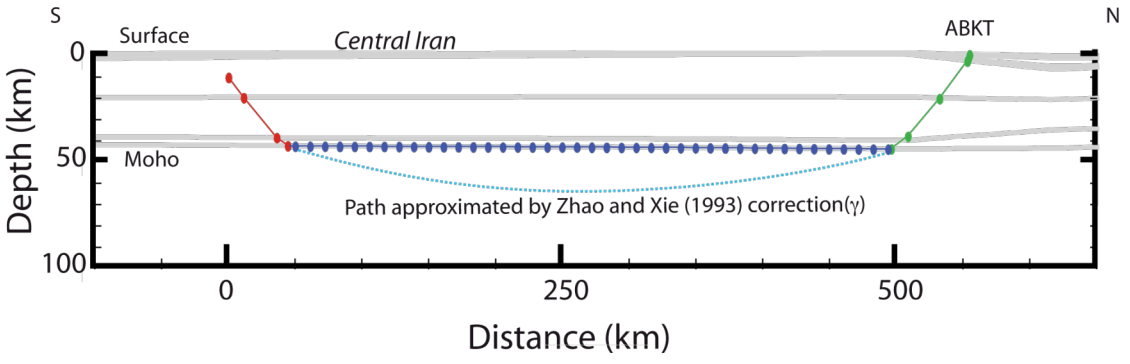

Figure 3. Cross section extracted from the laterally variable SLBM model. The components of the Pn/Sn travel-time calculation are also shown. The blue, red, green and cyan colors correspond to the first, second, third, and fourth terms of Eqn 1.

Travel-time accuracy

We use many approximations that enable on-the-fly, fast travel-time calculations. We test the accuracy of these calculations by comparing travel-times computed using the methods described above (SLBM) with travel-times computed using a fully 3-dimensional calculation described in Flanagan et al. (2007). The Flanagan et al. (2007) study uses the WENA1.0, 3-dimensional model of Pasyanos et al. (2004). We adopt the WENA1.0 crustal model and mantle velocity at the Moho discontinuity. We then compute the linear mantle gradient using the velocity at the Moho and the velocity at 130 km depth.

Figure 4 shows representative results of our tests. Figure 4a,b show the difference in Pn travel-times computed using the SLBM method and using 3-dimensional finite difference, respectively. In both cases the comparisons are relative to the iasp91 model, and Pn travel-times are computed using the TauP toolkit of Crotwell et al. (1999). The general features of Figure 4a and 4b are similar, with deviations from iasp91 travel-times ranging from approximately 2 seconds late to 6 seconds early. Figure 4c shows the difference between the SLBM and finite-difference calculations, with deviations between the two methods generally between plus and minus 1 second. Errors in the finite difference calculations themselves are reported to be approximately plus and minus 0.5 seconds (Flanagan et al., 2007), suggesting that the SLBM method is a good approximation to the full 3-dimensional calculation.

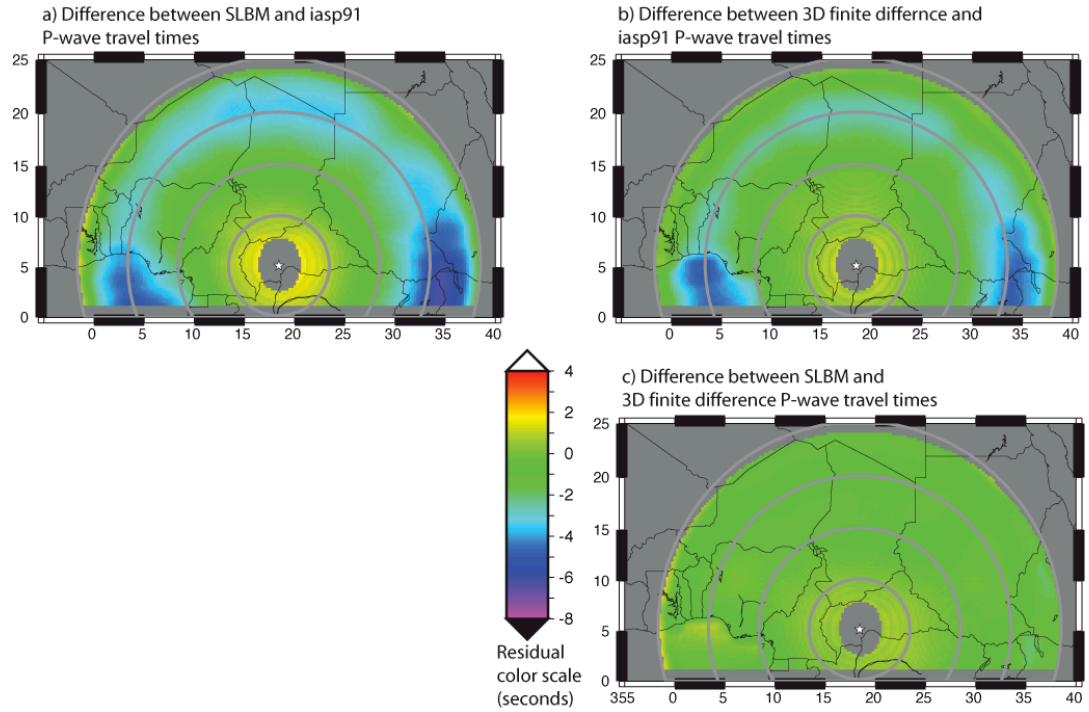

Figure 4. Comparision of Pn travel-times using SLBM and 3D finite difference calculations for station BGCA in central Africa. For SLBM and 3D finite-difference calculations the WENA1.0 model of Pasyanos et al. (2004) is used. Circles around the station are 5° increments. See text details.

Tomography

Test results presented above suggest that the SLBM travel-time method is in good agreement with 3-dimensional calculations. The WENA1.0 model used in the tests above is shown to improve travel-time prediction and location accuracy relative to the iasp91 default model (Flanagan et al., 2007). We further improve SLBM travel-time accuracy using tomographic methods.

A data set with small errors in event location and arrival-time measurements is critical to tomographic studies. Data coverage is also critically important. Lawrence Livermore (LLNL) and Los Alamos (LANL)

National Laboratories have combined ground-truth data sets for this study. Both national laboratories contribute global, regional, and local bulletins (some not widely available), as well as tens of thousands of arrival-time measurements made at the National Laboratories. All event locations are evaluated against Bondar et al. (2004) epicenter accuracy criteria, and all picks are evaluated against an error budget that accounts for event mislocation, iasp91 prediction error, and arrival-time measurement error. Observations outside of the 99% confidence bounds for total error are removed.

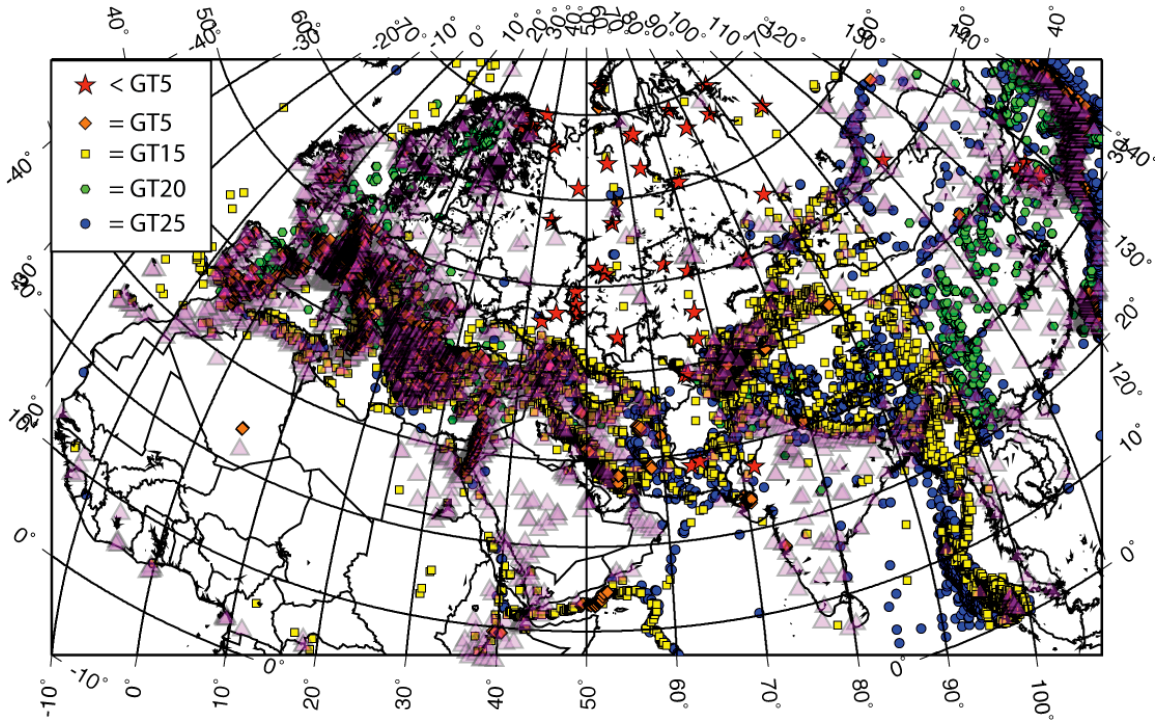

Figure 5. Tomographic data set. Purple triangles are stations with at least 1 regional-distance arrival-time measurement. Ground-truth location and accuracy (as defined in Bondar et al., 2004) are shown in the legend in the upper left. Regional ray coverage is excellent throughout the study area, with the exception of North Africa.

We are implementing the SLBM travel-time calculator into tomographic inversion programs. The general form of the tomographic inversion for Pn/Sn is as follows

$$T^k = \sum_{i=1}^{N} s_i^k x_i^k + \frac{\left(c^k\right)^2 \left(X_m^k\right)^3}{24 V_0} + \sum_{j=1}^{N} a_j^k \sum_{p=1}^{Q} \frac{l_p^k}{v_p^k} \qquad [8]$$

A significant difference between the formulation presented here and more typical Pn-tomography formulations is the introduction of a scalar value that adjusts the slowness of the crustal stack, as opposed to a static time-term to account for crustal travel-time delays. Adjusting the crustal slowness produces a model that is better suited to account for the effects of event depth on predict travel times, and therefore may better constrain event depth.

The tomographic free parameters are more easily described in matrix form

$$\begin{bmatrix} x_1^1 & \cdots & x_N^1 & -\frac{x_1^1 (X_m)^3}{24 V_O X_m} & \cdots & -\frac{x_N^1 (X_m)^3}{24 V_O X_m} & \sum_{p=1}^{Q} \frac{l_{1p}^1}{v_{1p}} & \cdots & \sum_{p=1}^{Q} \frac{l_{Np}^1}{v_{Np}} \\ \vdots & & & & \ddots & & & & \vdots \\ x_1^K & \cdots & x_N^K & -\frac{x_1^K (X_m)^3}{24 V_O X_m} & \cdots & -\frac{x_N^K (X_m)^3}{24 V_O X_m} & \sum_{p=1}^{Q} \frac{l_{1p}^K}{v_{1p}} & \cdots & \sum_{p=1}^{Q} \frac{l_{Np}^K}{v_{Np}} \\ & & & & & \text{Re}\,gularization & & & \end{bmatrix} * \begin{bmatrix} s_1 \\ \vdots \\ s_N \\ c_1^2 \\ \vdots \\ c_N^2 \\ a_1 \\ \vdots \\ a_N \end{bmatrix} = \begin{bmatrix} T^1 \\ \vdots \\ T^K \\ \text{Re}\,gularization \end{bmatrix}$$

where

T = *travel time*
s = *Pn slowness*
x = *Pn distance (or weight)*
c = *normalized velocity gradient v=vo(1+cz)*
Xm = *length of Pn path*
Vo = *average Pn velocity*
v = *velocity of a crustal layer*
k = *index on K paths (travel-time observations)*
i = *index on N model nodes (mantle path)*
j = *index on N model nodes (crustal path)*
p = *index on Q crustal layers*
a = *scalar adjustment to the crustal slowness stack at each node*

CONCLUSIONS AND RECOMMENDATIONS

This paper describes the progress of the SLBM project to date. This project is distinct because it tailors the travel-time prediction algorithm and tomography results to use in routine seismic location algorithms. Emphasis is placed on travel-time prediction accuracy and computational efficiency of regional phases.

The model parameterization provides global coverage and incorporates ellipticity. The current focus of the tomographic effort is Eurasia and North Africa, and the parameterization is easily extended to the globe. Further, the use of a tessellation approach allows fast interpolation of model parameters to extract the great-circle cross section of velocity structure that is needed to compute regional travel times.

We make use of several approximations that result in a relatively simple algebraic form for travel-time calculations. We have tested the accuracy of the approximate methods against a full, 3-dimensional finite-difference calculations. The differences between the approximate methods and full, 3-dimensional finite-difference methods are estimated to be less than 10% of errors observed by using a simple iasp91 background model. Therefore, we conclude that the approach developed here is a significant improvement in routine location practice.

We have developed an extensive quality controlled data set across Eurasia and North Africa. Further we are developing tomographic codes that are tailored to optimize the model parameters that are most important to seismic location.

ACKNOWLEDGEMENTS

This project would not be possible without the full support of Leslie Casey in the Department of Energy office of NA22. Steve Myers also wishes to thank Dave Harris for daily interactions and general technical discussions.

REFERENCES

Bondar, I., S. Myers, E. R. Engdahl, and E. Bergman, (2004). Epicenter accuracy based on seismic network criteria, *Geophys. J. Int.* **156,** no. 3, 483–496.

Flanagan, M.P., S.C. Myers, and K.D. Koper (2007). Regional travel-time uncertainty and seismic location improvement using a three-dimensional a priori velocity model, *Bull. Seismolog. Soc. Am*., **97**, 804-825.

Hearn, T. M. (1984). Pn travel times in southern California, *Jour. Geophys. Res*., **89**, 1843-1855.

Hearn, T.M., S. Wang, J.F. Ni, Z. Xu, Y. Yu, and X. Zhang (2004). Uppermost mantle velocities beneath China and surrounding regions, *J. Geophys. Res*., **109**, B11301, doi:10.1029/2003JB002874.

Helmberger, D.V. (1973). Numerical seismograms of long-period body waves from seventeen to forty degrees, Bull. Seismol. Soc. Am., 63, 633-646, 1973.

Kennett, B.L.N. and E.R. Engdahl, (1991). Traveltimes for global earthquake reference location and phase identification, *Geophys. J. Int,* **105**, 429-465.

Pasyanos, M.E., W.R. Walter, M.P. Flanagan, P. Goldstein, and J. Bhattacharyya (2004). Building and testing an a priori geophysical model for western Eurasia and North Africa, *Pure. And Applied Geophys*., **161**, 235-281.

Phillips, W.S., M.L. Begaud, C.A. Rowe, L.K. Steck, S.C. Myers, M.E. Pasyanos, and S. Ballard (2007). Accounting for lateral variations of the upper mantle gradient in Pn tomography studies, *Geophys. Res. Lett*. Revised.

Zhao, L.-S. (1993). Lateral variations and azimuthal isotropy of Pn velocities beneath Basin and Range province, *Jour. Geophys. Res*., **98**, 22,109-22,122.

Zhao and Xie (1993). Lateral variations in compressional velocities beneath the Tibetan Plateau from Pn traveltime tomography, *Geophys. J. Int*., **115**, 1070-1084.

This work was performed under the auspices of the U. S. Department of Energy by University of California, Lawrence Livermore National Laboratory under Contract W-7405-Eng-48.